A Micro-wires Based Tactile Sensor for Prosthesis

Guanhao Liang, Deqing Mei*, Yancheng Wang,
Yu Dai, and Zichen Chen

The State Key Laboratory of Fluid Power Transmission and Control,
Department of Mechanical Engineering,
Zhejiang University, Hangzhou, Zhejiang, 310027, China
medqmei@zju.edu.cn

Abstract. Tactile sensor is indispensable in prosthesis for object manipulation. This study presented a novel tactile sensor based on the conductive micro-wires that can measure the normal and shear forces. The developed sensor consists of four layers, from bottom to top are the substrate supporting, polyimide based matrix circuit, micro-wire based sensing, and top surface bump layers, respectively. To improve the sensing performance, structural dimensions were optimized. According to the optimization results, analytical models and finite element analysis (FEA) were conducted to study the normal and shear force sensing performance of the sensor. To develop the tactile sensor, the carbon-black based conductive polymer was firstly fabricated, and then the conductive micro-wires were manufactured by using the method of micro-contact printing (μCP). The results demonstrate that the machined micro-wires have dimensions of 250 μm in width and 50 μm in height.

Keywords: tactile sensor, normal force, shear force, micro-wires, prosthesis.

1 Introduction

The tremendous development of the prosthesis has proposed great demands for high-sensitivity flexible tactile sensors. Tactile sensor that capable of normal and shear force measuring is indispensable in prosthesis for object manipulation. To manipulate object, gentle touch is a very important function to determine whether the prosthesis get in touch with some object or not. With a high-sensitive tactile sensor, the prosthesis can perceive the environment as the skin of human being, which will largely improve the performance of gentle touch and tactile sensitivity.

So far, several kinds of tactile sensors have been developed with the sensing principles of piezoresistive [1-3], capacitive [4-5], piezoelectric [6-7], optical [8], etc. Organic field-effect transistors (OFETs), due to its flexibility and high sensitivity, have been preferred by researchers to develop flexible tactile sensor [9-11], especially with nano-wires field-effect transistors (NW FETs) [12] to amplify the sensing signals. In addition, there exist tactile sensor that compose of two sensing layers, which are capacitive layer to detect gentle touch and piezoresistive layer to detect

* Corresponding author.

J. Lee et al. (Eds.): ICIRA 2013, Part I, LNAI 8102, pp. 475–483, 2013.

common static force [13]. These studies have proposed many useful ways to increase the sensitivity of tactile sensor, but there still exists some problems to be solved, such as the flexibility. And the sensitivity of tactile sensor needs to be improved more to achieve better performance of the prosthesis.

Taking advantage of high sensitivity of the conductive micro-wires, this paper presented a micro-wire based tactile sensor to measure the normal and shear force. Structural optimization was conducted to improve the sensing performance. Then, analytical models and FEA were conducted to study the normal and shear forces measuring behavior. This was followed by the manufacture of the carbon-black based polymers. The conducted micro-wires were fabricated by the method of μCP [13-15]. Finally, the results and conclusions were conducted, respectively.

2 Design of the Tactile Sensor

As shown in Fig. 1, the designed tactile sensor mainly consists of four layers: substrate supporting layer, polyimide based matrix circuits layer, conductive micro-wires sensing layer, and top surface bump layer. One sensing element consists of four arrayed micro-wires with the substrate made of PDMS at 10:1 of monomer to curing agent, and laminated by a thin polyimide film, on which the matrix circuits are deposited by magnetron sputtering. The conductive micro-wires generated on the matrix circuits can measure the normal and shear forces. The total view of the tactile sensor is shown in Fig. 2, and the force applied on the surface of the bump can be decomposed into *Fx*, *Fy*, and *Fz* in *x*, *y*, *z* axis respectively.

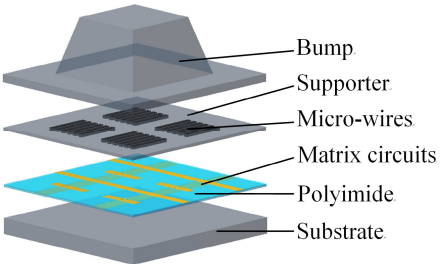

Fig. 1. Sensing layers of tactile sensor

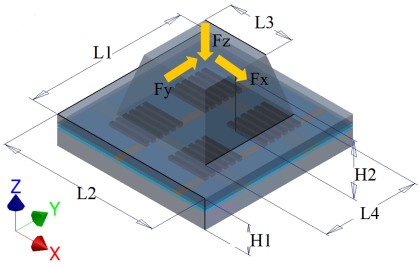

Fig. 2. Total view of the tactile sensor

The original state of the tactile sensor is shown in Fig. 3(a). When applying the normal force on the top surface bump, four micro-wires arrays will be compressed uniformly as shown in Fig. 3(b), which induces the decreasing of the resistivity of the micro-wires, thus can measure the normal force. When applying the shear force, two micro-wires arrays on the left side are stretched and the other two arrays on the right side are compressed, which lead to the increasing and decreasing of the resistivity of the micro-wires, respectively, as shown in Fig. 3(c).

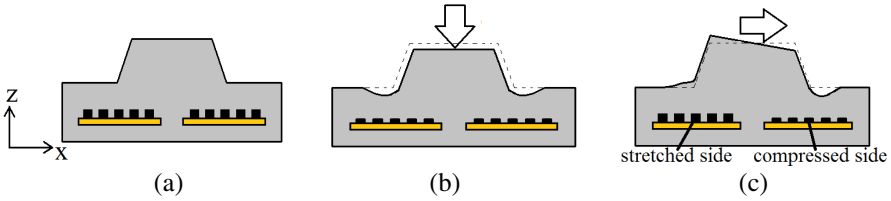

Fig. 3. Force sensing principle of the tactile sensor: (a) original state, (b) normal, and (c) shear force

3 Optimization and Modeling of the Tactile Sensor

To improve the sensing performance, structural dimensions of the tactile sensor need to be optimized. And according to the optimal dimensions, analytical models and finite element analysis (FEA) need to be conducted to establish relationship between the external force that applied on the tactile sensor and the forces that acting on the micro-wires.

3.1 Optimization of the Bump of the Tactile Sensor

The external forces are directly applied on the top surface bump, thus the dimensions of the surface bump are critical to the sensing performance of the tactile sensor. As shown in Fig. 2, one element of the tactile sensor is designed with dimension of 2 mm × 2 mm and with height of 0.36 mm. The bump is designed with height of 0.7 mm, the top square surface with dimensions of 0.82 mm × 0.82 mm. Totally, we can get dimensions $L1 = L2 = 2$ mm, $L3 = 0.82$ mm, $H1 = 0.36$ mm, $H2 = 0.7$ mm. The dimensions of the bottom surface bump $L4$ (as shown in Fig. 2) need to be optimized to increase the sensing performance of the sensor.

To optimize the surface bump geometry, FEA was conducted to find out an optimal $L4$ as shown in Fig. 2 using ANSYS software. With the optimal bump geometry, the micro-wires will be deformed largest when applying the same force, which means that the micro-wires are more sensitive to the force. The material properties values used in FEA model had been obtained by stretching and compression tests, as shown in Table. 1.

Fig. 4(a) and (b) show the average deformation in z direction of the micro-wires varies with the $L4$ of the bump when applying 0.5 N normal force in z direction and 0.5 N shear force in x direction, respectively. The deformation of the micro-wires increases as the $L4$ of the bump increase and reaches a peak value and then decrease. For the normal force, the peak value occurs at 1.3 mm (Fig. 4(a)), while for the shear force, the maximum deformation of the micro-wires I, III, and II, IV (Fig. 5(b)) occurs at $L4 = 1.2$ mm (Fig. 4(b)). When $L4$ of the bump is at small value, the

deformation of the micro-wires is mainly concentrated on the central area. As *L4* increase, the surface bump becomes larger, making the micro-wires receive less force and lead to a smaller average deformation. Thus, the peak value of the average deformation occurs at the optimal *L4* of the bump. From Figs. 4(a) and (b), the optimal *L4* of the bump equals 1.2 mm or 1.3 mm. In the following sections, *L4* that equals 1.2 mm will be adopted.

Table 1. Material properties used for FEA

Material	Young's modulus(Mpa)	Poisson's ratio
PDMS(7.5:1)	2.90	0.49
PDMS(10:1)	1.97	0.49
PDMS(20:1)	0.55	0.49
Polyimide	3500	0.34
Conductive micro-wires	2.90	0.49

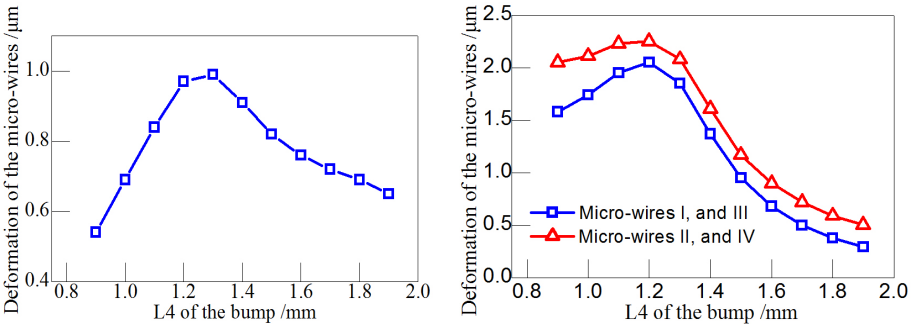

(a) Normal force (b) Shear force in *x* direction

Fig. 4. Dimension effects of the bump on the micro-wires deformation

3.2 Analytical Modeling of the Tactile Sensor

To measure the changes of the resistance of the micro-wires when the external force applied, analytical models need to be developed. Assuming the force is applied on the top surface of the bump, the force can be decomposed into three components: *Fx*, *Fy* , and *Fz* in *x*, *y*, and *z* directions, respectively, as shown in Fig. 5(a). *F1* , *F2*, *F3*, and *F4* are the forces acting on each of the micro-wires I, II, III, IV. Figs. 5(b) – (d) show the force component acting on each of the micro-wires when applying *Fx*, *Fy* , and *Fz* separately. F_{xj}, F_{yj}, and F_{zj} (j=1, 2, 3, 4) are the forces acting on the micro-wires when applying *Fx*, *Fy* , and *Fz* respectively.

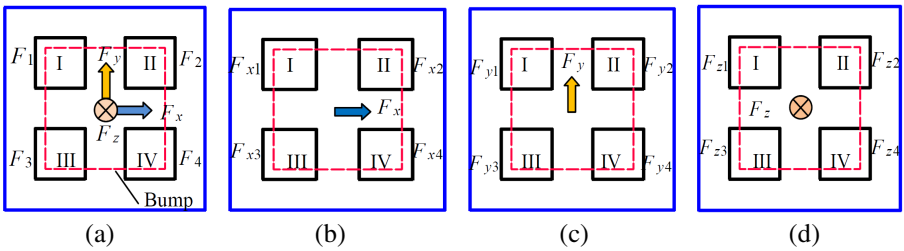

Fig. 5. Force distribution of the micro-wires when applying (a) 3D force, (b) *Fx* in *x* axis, (c) *Fy* in *y* axis and (d) *Fz* in *z* axis

As applying Fx, micro-wires I and III feature the same deformation, and micro-wires II and IV feature the same deformation as shown in Fig. 5(b). As applying Fy, micro-wires I and II feature the same deformation, and micro-wires III and IV feature the same deformation as shown in Fig. 5(c). And when applying Fz, micro-wires I, II, III, and IV feature the same deformation. Consider that the deformations of the tactile sensor are small, the tactile sensor can be considered as deforming linearly, so it can be inferred that there exists a linear relation between the force applied on the bump and the force acting on the micro-wires. So the following equations can be assumed:

$$\begin{cases} F_{x1} = F_{x3} = k_l F_x \\ F_{y1} = F_{y2} = k_u F_y \\ F_{x2} = F_{x4} = k_r F_x \\ F_{y3} = F_{y4} = k_d F_y \\ F_{z1} = F_{z2} = F_{z3} = F_{z4} = k_a F_z \end{cases} \tag{1}$$

where k_l, k_u, k_r, k_d, k_a are coefficients that are assumed and to be calculated though FEA.

According to the force superposition, Eq. 2 can be obtained:

$$F_{xj} + F_{yj} + F_{zj} = F_j \tag{2}$$

where j = 1, 2, 3, 4.

The relationship of the forces that acting on the micro-wires and their deformations can be expressed as:

$$F_{xi} = F_{yi} = F_{zi} = E \cdot \varepsilon \cdot S = E \cdot \frac{d_{DEF}}{l} \cdot S \tag{3}$$

where i = 1, 2, 3, 4; E is the Young's modulus of the micro-wires; ε is the average strain of the micro-wires; S is the top surface area of one array of the micro-wires; l is the height of the micro-wires; d_{DEF} is the deformation in z direction of the micro-wires.

To obtain the relationship between *Fi* (i = 1, 2, 3, 4) and *Fx, Fy , Fz* , FEA were conducted to calculate the coefficients k_l, k_u, k_r, k_d, and k_a. When normal force in z direction and shear force in x direction applied separately as shown in Fig. 5(b) and

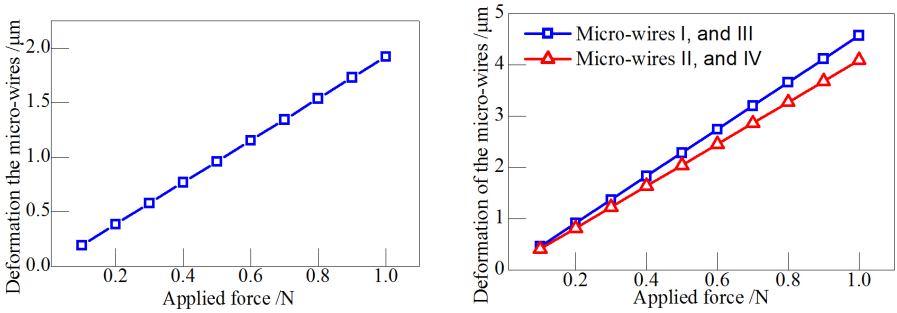

(a) Normal force (b) Shear force

Fig. 6. Force effects on the deformation of the micro-wires

(d), the deformations of the micro-wires are shown in Fig. 6. As the normal force increase, four micro-wires arrays deform linearly with the increasing of the normal force as shown in Fig. 6(a). From Fig. 6(b), micro-wires II and IV are compressed and micro-wires I and III are stretched, and they both deform linearly with the increasing of the shear force.

In this FEA, E = 3 MPa, S = 0.15 mm^2, and l = 100 μm. And the slope of the line in Fig. 6(a) can be expressed as follows according to Eqs. (1) and (3):

$$\frac{d_{DEF}}{F_z} = \frac{k_a \cdot l}{E \cdot S} = 1.922 \tag{4}$$

So k_a can be calculated from Eq. (4). In the same way, from Fig. 6(b) and Eqs. (1) and (3), k_l, k_u, k_r, k_d can be obtained as follows:

$$\begin{cases} k_a = 0.008649 \\ k_l = 0.02057 \\ k_u = 0.01340 \\ k_r = 0.01340 \\ k_d = 0.02057 \end{cases} \tag{5}$$

From Eqs. (1) – (5), the following expressions can be obtained:

$$\begin{cases} F_x = \dfrac{F_1 - F_2}{0.00717} \\ F_y = \dfrac{F_3 - F_1}{0.00717} \\ F_z = \dfrac{1.535F_2 - F_3}{0.004628} \end{cases} \tag{6}$$

where F_1, F_2, F_3 are the forces acting on micro-wires I, II, III.

From Eq. 6, the relationship between Fi (i=1, 2, 3, 4) and the force applied on the bump are developed. But we can notice that F_4 do not appear in Eq. (6), that's

because three arrays of micro-wires are already enough to calculate the force applied on the bump, and for the fourth micro-wires, its deformation can be used to increase the accuracy of the force measurement. The relation between *Fi* (*i*=1, 2, 3, 4) and resistance of the micro-wires can be linear in our designed range and it will not be discussed here. By measuring the *Fi* (*i*=1, 2, 3, 4) on each micro-wire array, the normal and shear forces can be calculated by using Eq. 6.

4 Fabrication of the Conductive Micro-wires

Nano-wires used in the tactile sensor have high sensitivity [12]. It can be inferred that if the conductive wires scale down to micron or even nanometer, they represent high sensitivity. Thus, the conductive micro-wires with high sensitivity are critical component of the designed tactile sensor. How to fabricate micro-wires that is as small as possible is challenging. This paper presents a μCP method [14-16] to fabricate the micro-wires.

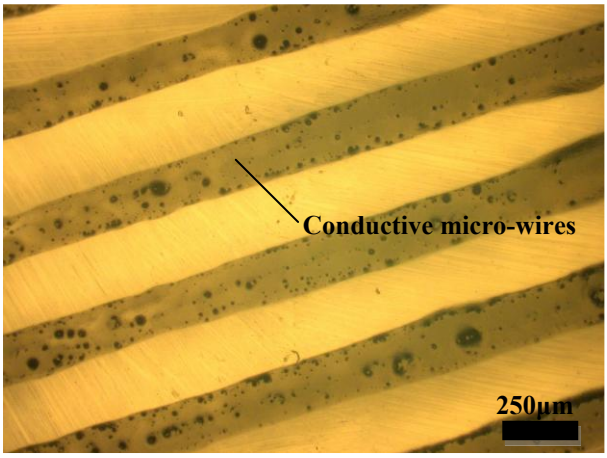

Fig. 7. Micro-wires fabricated on the slide glass

The fabrication process is as follows: 1) the carbon black with diameter of 30 nm were dispersed in toluene solution at 1:15 weight ratio, and magnetically stirred for 2 hours; 2) ultrasonic dispersion for 3 minutes to make the carbon black disperse more uniformly in toluene solution; 3) PDMS base polymer was added into toluene at 1:3 weight ratio, 4) these two solutions were mixed together and placed on magnetic stirring instrument (75 ºC) to evaporate the toluene completely, forming the liquid-state conductive polymer nano-composites; 5) the composite was spin coated on a silicon wafer; 6) a micro-wires patterned mold was placed on the composite thin layer for 10 seconds before lifting the mold up, leaving a thin layer of nano-composites on the patterns of the mold; 7) the mold was then stamped onto a slide glass to transfer the nano-composite pattern, forming the arrays of micro-wires on the slide glass; 8) then place the slide glass in the oven to cure the micro-wires at 80 ºC for 3 hours.

The fabricated micro-wires are shown in Fig. 7, the width and height of the micro-wires are 250 μm and 50 μm, respectively. Electrical characteristics will be tested in the future work.

5 Conclusions and Future Works

This paper presented a novel micro-wires based tactile sensor and μCP method to fabricate the micro-wires. The four micro-wires arrays using as the sensing element can measure the normal and shear force. To increase the sensing performance of the tactile sensor, the top surface bump geometries were optimized by using the FEA modeling. The optimal dimensions of the bump are 1.2 mm side length and 0.7 mm height. Based on the optimal surface bump, analytical models for the tactile sensor to measure the normal and shear forces were developed. The results show that the tactile sensor can measure the applied forces by measuring the resistance changes of the four micro-wires. To fabricate the micro-wires, μCP method and its fabrication process were proposed, the manufactured micro-wires features width of 250 μm and height of 50 μm. Conclusion can be drawn that micro-wire array based tactile sensor is feasible and can measure the normal and shear forces.

Future work will be to characterize the conductive ability of the micro-wires and sensing performance of the tactile sensor. Smaller micro-wires will be fabricated to achieve a higher sensitivity and utilized as the sensing element to develop a tactile sensor.

Acknowledgments. The author would like to acknowledge the supports from the National Basic Research Program (973) of China under Grant No. 2011CB013300, the National Natural Science Foundation of China under Grant No. 51105333, and the Postdoctoral Science Foundation of China under Grant No. 2011M500995.

References

1. Kim, K., Lee, K.R., Kim, W.H.: Polymer-based flexible tactile sensor up to 32×32 arrays integrated with interconnection terminals. Sens. Actuators A: Phys. 156, 284–291 (2009)
2. Noda, K., Hoshino, K., Matsumoto, K.: A shear stress sensor for tactile sensing with the piezoresistive cantilever standing in elastic material. Sens. Actuators A: Phys. 127, 295–301 (2006)
3. Yu, S., Chang, D., Tsao, L.: Porous nylon with electro-active dopants as flexible sensors and actuators. In: Proceedings of the IEEE 21st International Conference on Micro Electro Mechanical Systems (MEMS), Tucson, AZ, USA, pp. 908–911 (2008)
4. Lee, H., Chung, J., Chang, S.: Normal and shear force measurement using a flexible polymer tactile sensor with embedded multiple capacitors. J. Microelectromech. Syst. 17, 934–942 (2008)
5. Ying, M., Bonifas, A.P., Lu, N.: Silicon nanomembranes for fingertip electronics. Nanotechnology 23(34), 344004-1 (2012)

6. Hosoda, K., Tada, Y., Asada, M.: Anthropomorphic robotic soft fingertip with randomly distributed receptors. Robot Auton. Syst. 54, 104–109 (2006)
7. Dahiya, R.S., Valle, M., Metta, G.: Bio-inspired tactile sensing arrays. In: Proceedings of Bioengineered and Bioinspired Systems IV, Dresden, Germany, pp. 73650D-9 (2009)
8. Hoshino, K., Mori, D.: Three-dimensional tactile sensor with thin and soft elastic body. In: Proceedings of the IEEE Workshop on Advanced Robotics and Its Social Impacts, Taipei, Taiwan, pp. 1–6 (2008)
9. Mannsfeld, S.C.B., Tee, B.C., Stoltenberg, R.M.: Highly sensitive flexible pressure sensors with microstructured rubber dielectric layers. Nat. Mater. 9(10), 859–864 (2010)
10. Kawaguchi, H., Someya, T., Sekitani, T.: Cut-and-paste customization of organic FET integrated circuit and its application to electronic artificial skin. In: IEEE International Solid-State Circuits Conference, San Francisco, Canada, vol. 40(1), pp. 177–185 (2005)
11. Someya, T., Kato, Y., Sekitani, T.: Conformable, flexible, large-area networks of pressure and thermal sensors with organic transistor active matrixes. Proc. Natl. Acad. Sci. 102(35), 12321–12325 (2005)
12. Takei, K., Takahashi, T., Ho, J.C.: Nanowire active-matrix circuitry for low-voltage macroscale artificial skin. Nat. Mater. 9(10), 821–826 (2010)
13. Liang, G., Mei, D., Wang, Y., Dai, Y., Chen, Z.: Design and simulation of bio-inspired flexible tactile sensor for prosthesis. In: Su, C.-Y., Rakheja, S., Liu, H. (eds.) ICIRA 2012, Part III. LNCS (LNAI), vol. 7508, pp. 32–41. Springer, Heidelberg (2012)
14. Xia, Y.N., Whitesides, G.M.: Soft Lithography. Annu. Rev. Mater. Sci. 28, 153–184 (1998)
15. Zhong, C., Kapetanovic, A., Deng, Y.: A Chitin Nanofi ber Ink for Airbrushing, Replica Molding, and Microcontact Printing of Self-assembled Macro-,Micro-, and Nanostructures. Adv. Mater. 23, 4776–4781 (2011)
16. Chakra, E.B., Hannes, B., Dilosquer, G.: A new instrument for automated microcontact printing with stamp load adjustment. Review of Scientific Instruments 79, 64101–64102 (2008)